Physicochemical Studies of Kenaf Nanocrystaline Cellulose and Poly (3-hydroxybutyrate-*co*-3-hydroxyhexanoate) as Filler for Lithium Perchlorate based Polymer Electrolyte

M. Hazwan Hussin[1,], Nur Ain Tajudin[1], Nur Fatin Silmi Mohd Azani[1], Murugan Paramasivam[2], M. K. Mohamad Haafiz[2], Sudesh Kumar[3], Mehdi Yemloul[4]*

[1] School of Chemical Sciences, Universiti Sains Malaysia, 11800, Minden, Penang, Malaysia.
[2] School of Industrial Technology, Universiti Sains Malaysia,11800, Minden, Penang, Malaysia
[3] School of Biological Sciences, Universiti Sains Malaysia, 11800, Minden, Penang, Malaysia.
[4] AMU iSm2 Service 512, Campus Scientifique de St Jérôme, 13397 Marseille, France
[*]E-mail: mhh@usm.my; mhh.usm@gmail.com

Solid state polymer electrolyte attracts a great attention due to its thermal stability, no leakage, excellent flexibility, and good processability. There are many polymers have been investigated for electrochemical device applications. This study aims to evaluate the efficiency of polymer electrolyte consists of PHA (Biologically recovered and purified poly (3-hydroxybutyrate-*co*-25% 3-hydroxyhexanoate) (P(3HB-*co*-25% 3HHx)) and lithium perchlorate (LiClO$_4$) for the first time. On the other hand, nanocrystalline cellulose (NCC) was also used as filling material, which was extracted from soda kenaf pulp *via* acid hydrolysis. Then extracted NCC was characterized by XRD, TEM, BET, 13C NMR, SEM, TEM, FTIR, and TGA. The results showed that the NCC extracted from soda kenaf pulp have high crystallinity index. Finally, Polymer electrolyte was prepared by film casting method using NCC, biologically recovered P(3HB-*co*-25% 3HHx) with different percentage of LiClO$_4$ ((0, 10, 20, 30, and 40% (w/w)). Prepared thin films were analysed using cyclic voltammetry (CV) and electrochemical impedance spectroscopy (EIS). The results from CV and EIS analyses confirmed that the polymer electrolyte consists of 40 % LiClO$_4$ showed the highest conductivity of 1.56×10^{-4} S cm^{-1}.

1. INTRODUCTION

Nowadays, with the fast development of technologies globally, the requirement of higher performance of energy sources has really garnered a lot of interest. One of the technologies that have

generated a remarkable interest in the polymer-based ion conducting materials. This is mainly due to their application as an electrolyte that functions as a separator between two electrodes and the ionic conduction medium. Mostly, these are used in the form of thin films or plasticized electrolytes. The ionic conductivity of the polymer electrolyte is enhanced by adding suitable filling materials [1]. Previously, many studies have been carried out by using various types of fillers combined with host polymers such as poly(vinylidene fluoride-hexafluoropropylene) copolymer, poly(acrylonitrile), poly(ethylene oxide) and poly(methyl methacrylate)[2]. However, these are not bio-based polymers. Therefore, the researcher looks for the natural biodegradable polymers from renewable resources to replace the synthetic non-biodegradable polymer. Polyhydroxyalkanoates are the bio-based polymer produced by the microorganisms and it is 100% biodegradable. Certainly, PHA has better mechanical property, film-forming ability, resistance and electrochemical stability [3]. The stability of PHA can be improved by blending other polymers such as cellulose [4]. On the other hand, the polymer blend with $LiClO_4$ salt increases the amorphousness and conducting ionic species in the polymer membrane [5].

From the cellulose, nanocellulose could be extracted via a chemical reaction. The nano-sized cellulose has a lot of advantages. To be more definite, cellulosic nanofillers are comprised of nanosized cellulose with typical measurement of 4nm to 20nm laterally and longitudinal dimension ranging from nanometer to micrometer [6]. Cellulose nanofiller is possible to produce in large scale, it has a high surface to volume ratio, ease of chemical modification and high mechanical strength. Apart from that, it is also environmentally friendly and has high renewability prospect. The addition of nanofillers into nanocomposites drastically increases the thermal, mechanical and fire retardant properties [6].

In order to isolate the cellulose nanocrystal, a method like acid hydrolysis could be used. After obtaining the cellulose from the plant by pulping, bleaching and mercerization, the cellulose obtained would have to be dissolved in sulphuric acid [7]. Thus, the aim of this research is to study the ionic conductivity and physicochemical properties of the $NCC-PHA-LiClO_4$ composite as the potential polymer electrolyte which is biodegradable and biocompatible. The NCC extracted from kenaf pulp was characterized by using the X-ray diffraction (XRD) spectroscopy, N_2 adsorption of Brunaeur-Emmett-Teller (BET), cross polarization magic angle spinning nuclear magnetic resonance (CP/MAS ^{13}C NMR), Fourier Transform Infrared Spectroscopy (FTIR), scanning electron microscopy (SEM) and thermal behavior. Different percentage of $LiClO_4$ ((0, 10, 20, 30, and 40% (w/w)) with NCC and P(3HB-*co*-25% 3HHx) was prepared by the film casting method and characterized. The prepared polymer electrolyte was evaluated for its ionic conductivity using electrochemical impedance spectroscopy (EIS) and cyclic voltammetry (CV).

2. MATERIALS AND METHODS

2.1 Materials

The Kenaf used is the commercialized sun-dried, grounded and sieved powder which was obtained from the Finaf Industries Sdn. Bhd., Kedah. The ground Kenaf was dried at 50 ˚C for 24 hours in a hot air oven. Then, the Kenaf powder undergoes extraction analysis *via* Soxhlet extractor using the mixture of ethanol-toluene at the ratio of 2:1 at 70 ˚C for 5 h [7]. The Kenaf powder used in this

experiment consists of 22.70% (w/w) hemicelluloses, 28.85% (w/w) cellulose, 89.2% (w/w) extractives, 0.3% (w/w) moisture content, 2.4% (w/w) ash content and 22.2% (w/w) Klason lignin on a dry weight basis. Poly(3-hydroxybutyrate-*co*-25% 3-hydroxyhexanoate) *(*P(3HB-*co*- 25% 3HHx)) was produced by the recombinant strain *Cupriavidus necator* Re2058/pCB113 using palm olein as the sole carbon source. Produced PHA was biologically recovered and purified using detergents [8].

2.2 Chemicals

Chemicals used in this study was Hydrochloric acid, 37% HCl (QRec, Malaysia), Acetic Acid, HOAc (QRec, Malaysia), Sulphuric Acid, H_2SO_4 (QRec, Malaysia), Toluene, C_7H_8 (QRec, Malaysia), Sodium Hydroxide pellets, NaOH (QRec, Malaysia), Ethanol, EtOH (QRec, Malaysia), Methanol, MeOH (QRec, Malaysia), Sodium Sulfide , Na_2S (QRec, Malaysia), Sodium Chlorite , $NaClO_2$ (Sigma-Aldrich, United States), Glycerol, $C_3H_8O_3$ (HmbG, Malaysia) and Lithium Perchlorate, $LiClO_4$ (Sigma-Aldrich, United States). Distilled water was used to prepare all the reagents.

2.3 Soda pulping

A 10 L steel reactor was used for the Soda pulping process. The conditions used for the soda pulping process by maintaining at the ratio of 1: 8 (Kenaf: water) with 20% active alkaline and 30% sulfidity. The pressure was set at a range of 12-15 bar. The pulping process was carried out at 170 ˚C for 3 hours. Finally, the pulp was filtered out using a vacuum filtration process and dried under the sun until constant weight [9].

2.4 Pulp bleaching

In order to obtain the holocellulose from the Kenaf pulp. The bleaching process was carried out. Through the bleaching process, the remaining lignin will be removed or decolorized thus enhancing the physical and optical qualities. Without degrading the cellulose, the pulp was reacted with sodium chlorite. The isolation process of the holocellulose began by mixing 4.5 g of the pulp in 125 mL deionized water, add 3.0 mL of glacial acetic acid and 3.0 mL of sodium chloride. This mixture is heated at 70 ˚C for 2 h with constant stirring [10] . After the heating process, the holocellulose was filtered and washed with distilled water. Finally, the holocellulose was dried at 50 ˚C for 24 h in a hot air oven. The percentage of holocellulose obtained from the pulp bleaching process was calculated using the formula below:

$$\% \, Holocellulose = \left[\frac{Holocellulose \, Mass(g)}{Initial \, OPF \, Mass(g)} \right] \times 100 \qquad (Eq.1)$$

2.5 Mercerization of the Holocellulose

The reaction was carried out using 2.0 g of dried holocellulose sample with 100 mL of 10% (w/v) of NaOH for 30 min. After the 30 minutes, 100 mL of distilled water was added with continuous stirring for another half an hour at room temperature. The cellulose obtained from this process was filtered and washed with 1% (w/v) HOAc, 5 % (w/v) NaOH and distilled water. The washed cellulose was dried at 50 ˚C for 24 h in a hot air oven. The percentage of holocellulose and hemicellulose obtained from this process was calculated using the formula below:

$$\% \ Cellulose = \left[\frac{Cellulose \ Mass(g)}{Initial \ OPF \ Mass(g)} \right] \times 100 \qquad (Eq.2)$$

$$\% \ Hemicellulose = \% \ Holocellulose - \% \ Cellulose \qquad (Eq.3)$$

2.6 Acid Hydrolysis

The obtained cellulose was then further treated with acid hydrolysis to produce Nanocrystalline cellulose. About 2.0 g of the cellulose was dissolved in 17.5 mL of 50% H_2SO_4 at room temperature for almost 30 minutes with constant stirring. Then, the hydrolysis process was stopped by adding about 87.5 mL of cold water. The solution was centrifuged at 7960 rpm for 10 mins (4 times). Finally, the pH was neutralized by transferring the nanocrystalline cellulose was transferred to the dialysis tube. The dialysis process was stopped when the solution reaches the pH 7 [11].

2.7 Preparation of the polymer electrolyte

The film casting method was used to produce the composite of the polymer electrolyte. About 2.7 g of PHA was weighed and dissolved in 30 mL of chloroform. This solution was stirred for 30 mins. Further, this solution added with 0.3 g of nanocrystalline cellulose, 0.5 g glycerol and different percentage of lithium perchlorate (soda NCC-PHA-0 % $LiClO_4$, soda NCC-PHA-10 % $LiClO_4$, soda NCC-PHA-20 % $LiClO_4$, soda NCC-PHA-30 % $LiClO_4$, and soda NCC-PHA-40 % $LiClO_4$ (w/w)). The composite mixture was stirred for another 30 mins to obtain a uniform suspension. Finally, the solution was poured into the petri dish and covered with aluminium foil with holes. The Petri dishes were kept under the fume hood for 48 hours to evaporate the chloroform. The PHA film composite was peeled-off from the petri dish. The thickness of the film was measured using the Vernier Caliper [12].

2.8 Characterization

2.8.1 FTIR analysis

The functional group of microcrystalline cellulose and nanocrystalline cellulose was analyzed using Fourier Transform Infrared Spectroscopy (FTIR) (Perkin-Elmer System 2000 spectrometer) by

mixing the sample with KBr at the ratio of 1:10. The range of spectra was taken between the wavenumber of 4000-400 cm^{-1}. The sample was scanned for 20 times and the spectra were recorded.

2.8.2 CP/MAS ^{13}C NMR analysis

The cross-polarization magic angle spinning (CP/MAS) measurements were taken using solid-state nuclear magnetic resonance (Bruker Avance 400 MHz spectrometers) with the frequency of 76.46 MHz. The samples were scanned for 10,000 times and the spectra were recorded. The cylindrical zirconia rotors were used to press the samples and spun at a magic angle at 7 kHz.

2.8.3 XRD analysis

X-ray diffraction (XRD) pattern of microcrystalline cellulose and nanocrystalline cellulose was measured using PANalytical X'Pert PRO MRD PW 3040. The Cu-Kα radiation was used to measure the diffraction patterns at 40 kV and 35 mA. The nanocrystalline cellulose was pelletized into 25 mm diameter by compressing under the pressure of 50 MPa. The crystallinity index of nanocrystalline cellulose was calculated using the Eq.4.

$$\% \ CrI = \frac{I_{002} - I_{am}}{I_{002}} \times 100 \qquad \qquad \text{(Eq.4)}$$

Where *CrI*, crystallinity index; I_{002}, the peak intensity of the 002 lattice plane (about $2\theta = 22.0°$) and I_{am}, peak intensity of the amorphous phase (about $2\theta = 17.0°$ and $18.0°$) for type I cellulose.

2.8.4 Thermal behavior

Thermal stability of nanocrystalline cellulose and cellulose were analyzed using thermogravimetric analyzer (Perkin-Elmer TGA 7). The samples were heated from the temperature range of 30 to 900 °C at a heating rate of 10 °C min^{-1}. The melting temperature was determined using Differential scanning calorimeter (DSC) (Perkin Elmer Pyris 1). The samples were heated from 300 to 400 °C at a heating rate of 10 °C min^{-1}.

2.8.5 Surface and morphology analysis

The samples were analyzed to obtain the external surface area, BET surface area, total pore volume and pore size by using a Quantachrome Nova Win2© 1994-2002. The surface morphology the samples were analyzed using Transmission Electron Microscopy (TEM) (Philips CM12) equipped with an image analysis system (Docu' ver 3.2).

2.8.6 Electrochemical properties

The films prepared were tested for its ionic conductivity using a Gamry Reference 600 potentiostat impedance unit. The samples were scanned AC frequency from 1 MHz to 1 Hz at 10 mV amplitude. The film samples prepared was placed in between the stainless-steel electrodes. The data obtained from this analysis was fitted to an equivalent circuit using Echem Analysis. The ionic conductivity of the film samples was calculated by using the formula mentioned below:

$$\sigma = \frac{L}{R_b A} \qquad \text{(Eq.5)}$$

Where L is film thickness (cm), R_b is the bulk resistance of the polymer electrolyte (Ω cm^2) and A is the exposed area of the polymer electrolyte (3.142cm^2). The electrochemical stability of the polymer electrolyte was measured from the electrochemical window. In this experiment, the analysis of the polymer electrolyte using cyclic voltammetry (BASi Epsilon-EC potentiostat). The solid-state polymer electrolyte was placed between two stainless steel electrodes. The cyclic voltammetry was set to have a voltage at -1 V to +1 V with a scan rate of 10 mV s^{-1}.

3. RESULTS AND DISCUSSION

3.1 Extraction of cellulose

The results showed that the extraction process yields from soda pulping process consist of 63.0 $\pm$ 0.5 %, 17.32 $\pm$ 0.2 % holocellulose and remaining 45.68 $\pm$ 0.2 % hemicelluloses and cellulose (Fig. 1).
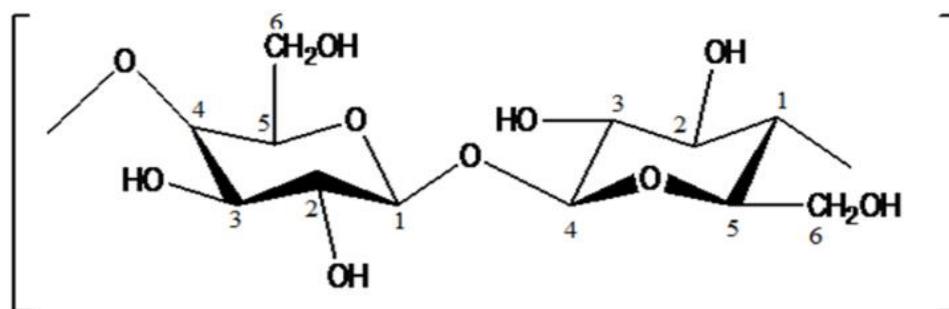

Figure 1. The structure of cellulose

3.2 FTIR analysis

FTIR spectra of soda NCC and soda cellulose sample are shown in Fig. 2. The vibrational assignments are summarized in Table 1. FTIR analysis revealed that the peak obtained from all the samples were similar which indicated all the samples consist of the same chemical composition. The results obtained from FTIR analysis compared with the spectra of pure cellulose reported elsewhere [7,13,14]. The stretching of –OH groups confirmed from the broad peak obtained around the wavenumber 3300 to 3500 cm^{-1} and the CH$_2$ groups showed the peak between the 2800 to 3000 cm^{-1}

[15]. Besides that, the strong interaction between cellulose and water was confirmed by the peak absorption around the wavenumber 1646 cm^{-1} which indicates the bending of water molecules. The peak obtained at 1431 cm^{-1} refers to CH_2 bending that indicates the increase in nanocrystalline cellulose structure. The intensity of this peak expresses the crystallinity, the higher the intensity indicates the higher degree of crystallinity. Meanwhile, the C-O-C stretching refers to the peak absorption around 1163 to 1200 cm^{-1} indicates and the peak around 895 to 900 cm^{-1} are associated to C-H rock vibration of cellulose (anomeric vibration of β-glucosides) observed in soda NCC and micro cellulose samples [16]. The complete removal of lignin was confirmed by the absence of peak between the wavenumber 1509 to 1609 cm^{-1} which correspond to C=C aromatic skeletal vibration [15,17] and the removal hemicellulose was confirmed from the absence of peak in the region of 1700 to 1740 cm^{-1} which belong to uronic ester or acetyl groups [18]. The results suggested that the NCC obtained from the process of hydrolysis was pure cellulose.

Table 1. FTIR spectral peak assignments for Soda cellulose and Soda nanocrystalline cellulose

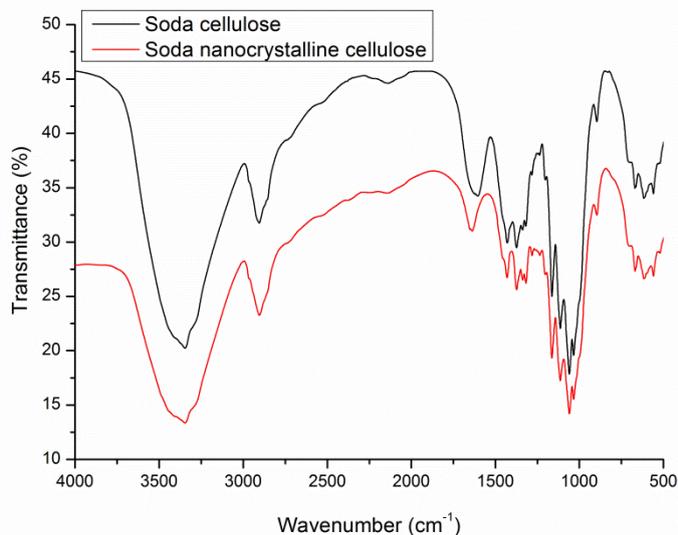| Wavenumber (cm^{-1})	Peak assignments
3300-3500	-OH stretching
2800-3000	CH_2 groups
1646	O-H bending
1431	CH_2 bending
1163-1200	C-O-C stretching
895-900	C-H rock
801	C-H bending and ring puckering

Figure 2. FTIR-spectra of Soda cellulose and Soda nanocrystalline cellulose

3.3 CP/MAS ^{13}C NMR analysis

      The structure of NCC extracted from soda pulping process was confirmed by CP/MAS ^{13}C NMR analysis (Fig. 3). The peaks obtained from the analysis was assigned based on the literature [19,20]. The arrangement of different carbon in the cellulose was confirmed from the peaks between 59 to 106 ppm. In NMR spectra of soda-NCC showed that the group of resonance between 70-75 ppm belongs to the carbon of C2, C3 and C5 and the resonance at the region of 104,106 ppm corresponds to the carbon of C1[21]. The peaks anticipated at the region of 65-69ppm are belonging to the carbon of C6. Besides that, the resonance peak in the amorphous region of 62-64 ppm referred to the carbon of C6. The C4 carbon was confirmed from the signals between 86 to 92 ppm due to crystalline form along with paracrystalline regions. The region of broader up field resonance between 80 to 86 ppm indicates the amorphous region.
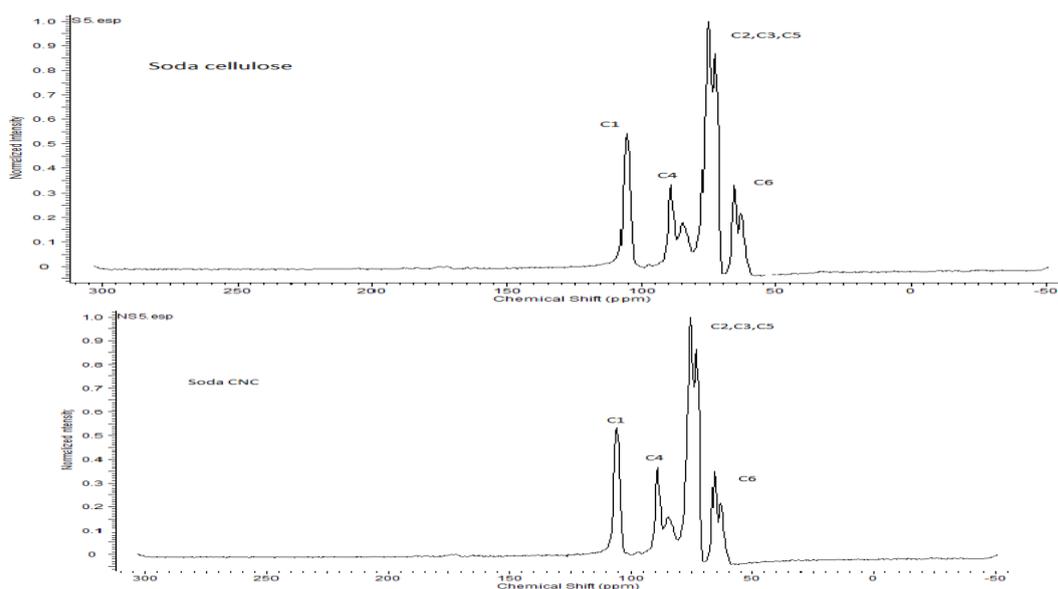

Figure 3. Solid state CP/ MAS ^{13}C NMR spectra of Soda cellulose and Soda nanocrystalline cellulose

3.4 XRD analysis

      The X-ray diffraction patterns of NCC samples prepared from soda Kenaf is shown in Fig. 4. The crystallinity index calculated for the different samples are shown in Table 2. The diffraction peaks of 2θ angles between 18.0˚ to 22.0˚ were comparable to the typical diffraction pattern of cellulose I. This result indicates that the nanocrystalline cellulose extracted from the Kenaf fiber consists of cellulose type I (22.0˚, 002 lattices). The diffraction peak becomes sharper at 22.0˚ confirms that the increase in crystallinity. The crystallinity of extracted cellulose increased to 70% due to the acid hydrolysis treatment. The results revealed that the remaining hemicellulose in cellulose was completely dissolved and the interactions were disturbed between lignin-hemicellulose-cellulose [7]. which later contributes to the individual crystallinities [16]. All the data obtained from XRD indicates that the samples consist

of crystalline native cellulose I. Apart from that, acid hydrolysis treatment yields the cellulose with high purity without the degradation [7].

Table 2. Crystallinity index, *CrI (%)* of Soda cellulose and Soda nanocrystalline cellulose

Sample	Lattice plane, I_{002}	Amorphous phase, I_{am}	Crystalinity index, *CrI (%)*
Soda cellulose	1551	413	51%
Soda NCC	1689	399	70%
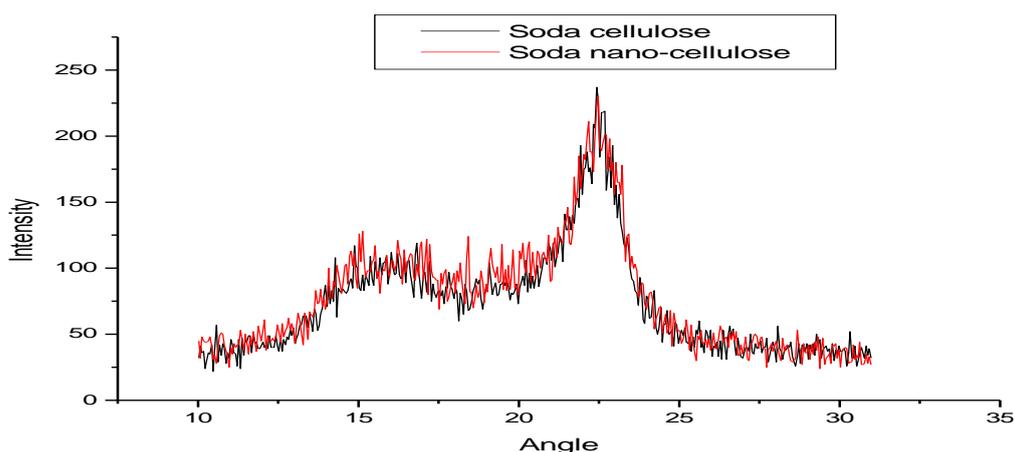
Figure 4. X-ray diffraction pattern of Soda cellulose and Soda nanocrystalline cellulose

3.5 Thermal analyses

Thermal stability of the samples was determined by the weight loss after heating over the high temperature using Thermal gravimetry analyzer (TGA) and derivative thermograms (DTG). The TGA thermogram obtained from the samples shown in Fig.5. The weight loss observed in two stages when the samples heated from 30 ˚C to 900 ˚C. Initially, the weight loss observed in the region of 60-100 ˚C due to the elimination of water molecules within cellulose. Meanwhile, the major weight loss was observed at the temperature between 250-450 ˚C. The weight loss of cellulose due to the decomposition of glycosyl units. It is anticipated that the NCC should have higher weight loss after acid hydrolysis treatment. The higher thermal stability may be due to the higher purity of microcrystal-sized cellulose [13]. The melting temperature (T_m) of soda-NCC obtained from DSC analysis (Data not shown). DSC results revealed that the melting temperature of soda-NCC was 160.19 ˚C. According to the results obtained suggested that the NCC extracted from kenaf possesses high thermal stability. Hence it can be used in bio-composite, food stabilizer and pharmaceutical compounds [7].
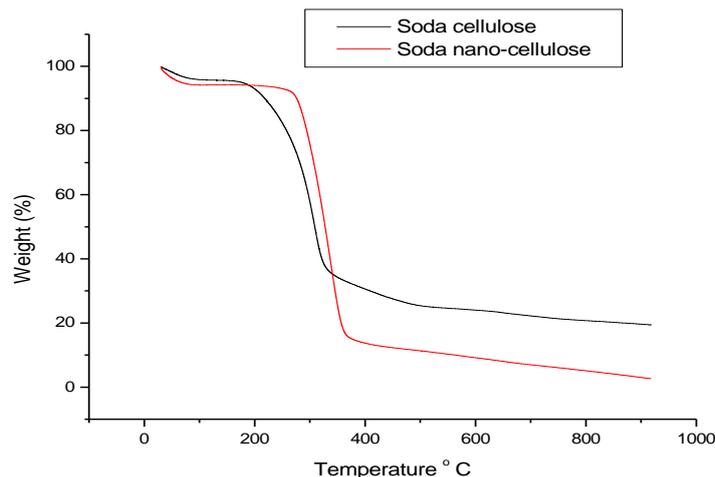
Figure 5. TGA thermograms of Soda cellulose and Soda nanocrystalline cellulose

3.7 Surface and morphology analysis

The results obtained from surface and morphology analysis (BET) are shown in Table 3. The results showed that the improvement in BET surface area after the acid hydrolysis treatment. The extracted soda-NCC can be classified as microporous based on the average pore width (0.934 nm). The results from BET surface area analysis revealed that the diameter of microporous materials was around <2 nm, pore diameter of mesoporous materials between 2 to 50 nm and disperse, nonporous or the pore diameter of macroporous materials is >50 nm. The surface morphology of soda-NCC was further investigated by TEM analysis (Fig. 6) TEM analysis revealed that the size of the crystal obtained from the extraction process in nanometre with an average of 169.32 nm. The incorporation of extracted NCC in the film enhances the ease of chemical modification, high surface to volume ratio and high mechanical strength [6].

Table 3. Characteristics of Soda nanocrystalline cellulose obtained by BET Analysis

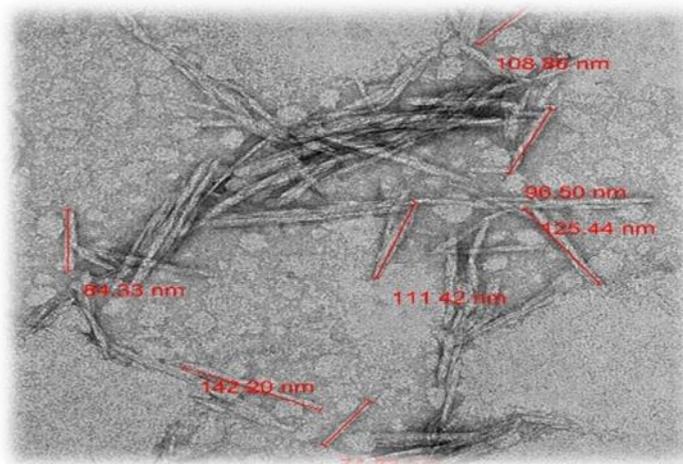| Sample	BET surface area $(m^2\ g^{-1})$	Total pore volume $(cm^3\ g^{-1})$	Cumulative pore volume $(cm^3\ g^{-1})$	Average pore width (nm)
Soda NCC	5.0850	0.001896	0.0213	0.934

Figure 6. TEM image of Soda nanocrystalline cellulose

3.8 Electrochemical studies of the polymer electrolyte.

The bulk ionic conductivity is one of the important parameters to evaluate the polymer electrolyte. The results obtained from EIS were calculated by fitting it with an equivalent electrical circuit (Fig. 7). The polymer electrolyte prepared in the form of film containing NCC-PHA-LiClO$_4$ with the different percentage of LiClO$_4$ and analyzed for its ionic conductivity from the complex impedance spectra (Fig. 8 a and b). The ionic conductivity values of the of the polymer electrolyte are compiled in Table 4. The results revealed that the ionic conductivity of the polymer electrolyte increases when the LiClO$_4$ concentration was increased from 0% to 40%. The reason for the increase in ionic conductivity could be due to the amount of the charge carriers increased in the polymer electrolyte system. In addition, the ionic conductivity also relies upon the mobility together with polymer chain mobility or the polymer segmental mobility [2]. The lithium ions act as a charge carrier in the polymer electrolyte. It suggests that the conductivity correlates with the presence of lithium ions.

The lithium ions are the most probable species for carrying charges in polymer electrolytes and the conductivity corresponds to the present of Li$^+$ ions. The higher ionic conductivity was found to be 1.56×10^{-4} S cm^{-1} for the film containing NCC- PHA-40% LiClO$_4$. While the ionic conductivity for PHA-40% LiClO$_4$ (without NCC) is 1.67×10^{-5} Scm^{-1}. The higher conductivity of PHA polymer could be due to the properties of PHA filler which related to the low molecular weight and the high degree of crystallinity that promotes better ion transport.

The working voltage range of the polymer electrolyte was estimated using cyclic voltammetry (CV). The results output from cyclic voltammetry will use for making the decision for further application of polymer electrode in electrochemical devices such as batteries. The CV pattern of the film consists of Nano crystalline cellulose (NCC), Polyhydroxyalkanoates (PHA) and Lithium perchlorate (LiClO$_4$) was shown in Fig. 9. The results revealed that the electrochemical stability window potential of the film consists of NCC- PHA-0% LiClO$_4$ was around 0.1 V and NCC-PHA-40% LiClO$_4$ was 0.75 V.

Table 4. The parameters of ionic conductivity for composite polymer of soda-NCC.

Sample	Thickness, $\times 10^{-3}$ (cm)	$R_b, \times 10^x$ (Ω cm^2)	Conductivity, σ (S cm^{-1})
soda NCC-PHA-0% LiClO$_4$	0.63	17.46×10^6	5.10×10^{-9}
soda NCC-PHA-10% LiClO$_4$	0.60	5.34×10^3	1.59×10^{-5}
soda NCC-PHA-20% LiClO$_4$	0.55	549	1.42×10^{-4}
soda NCC-PHA-30% LiClO$_4$	0.55	1.96×10^3	3.97×10^{-5}
soda NCC-PHA-40% LiClO$_4$	0.47	425.73	1.56×10^{-4}
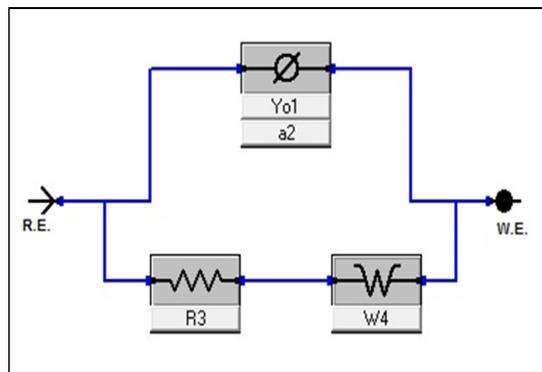
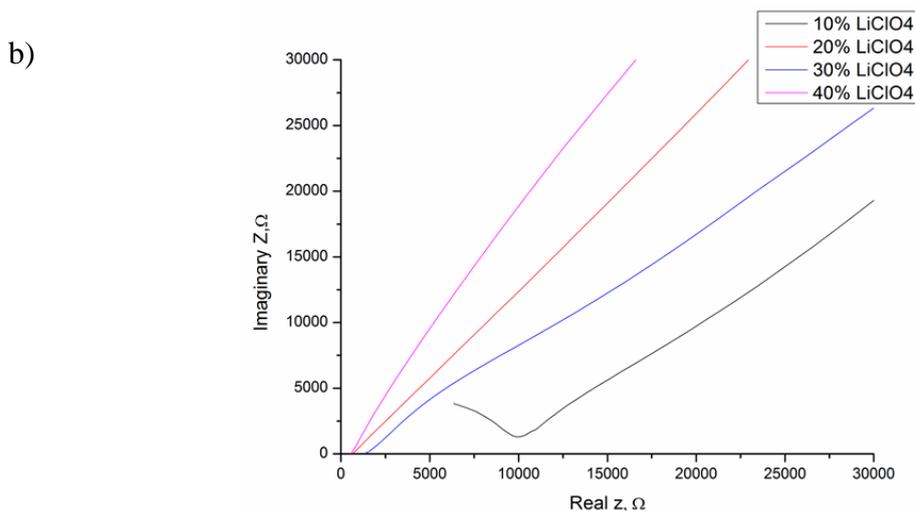**Figure 7.** An equivalent electrical circuit used for electrochemical impedance spectroscopy (EIS) fitting

b)
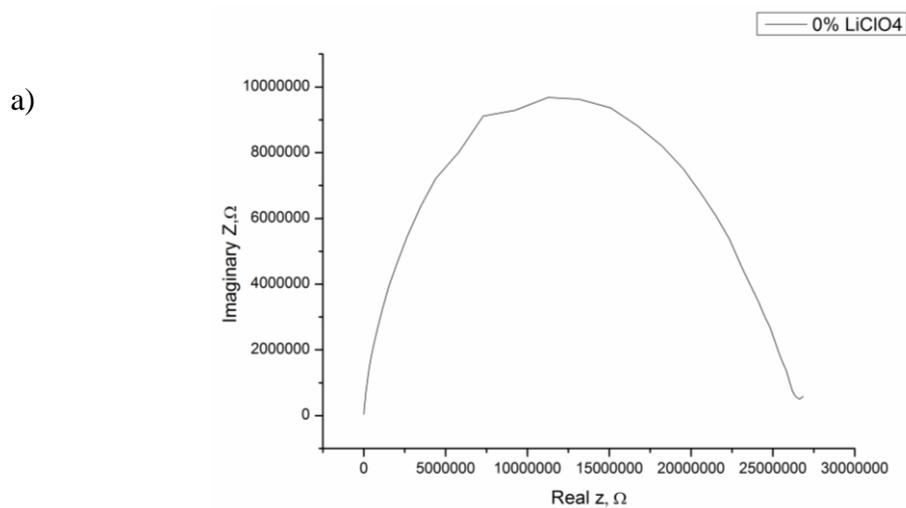
Figure 8. Nyquist plots of a) soda NCC-PHA-0 % LiClO$_4$ and b) Different percentage of LiClO$_4$ (10%, 20%, 30% and 40%) in soda NCC-PHA-LiClO$_4$ film
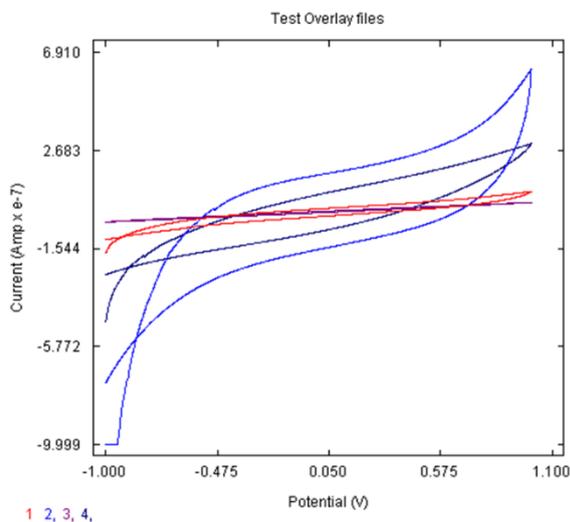

Figure 9. The overlay of cyclic voltammetry curves of the NCC-PHA-LiClO$_4$ polymer electrolyte film.

4. CONCLUSION

Nanocrystalline cellulose has been successfully isolated using acid hydrolysis treatment. Finally, Polymer electrolyte was prepared by film casting method using NCC, biologically recovered P(3HB-*co*-25% 3HHx) with different percentage of LiClO$_4$ ((0, 10, 20, 30, and 40% (w/w)). The ionic conductivity of the prepared film was increased by increasing the salt concentration. A maximum conductivity was found to be 1.67×10^{-5} S cm^{-1} for the film consist only P(3HB-*co*-25% 3HHx)-40% LiClO$_4$ with electrochemical stability window potential around 1.7 V. The highest ionic conductivity of the PHA-based fillers in polymer electrolyte is suited well for their further applications especially in the performance of Li-ion batteries.

References

1. M.A.S.A. Samir, F. Allein, W. Gorecki, J.-Y. Sanchez, A. Dufresne, *J. Phys. Chem. B*. 108 (2004) 10845–10852.
2. J. Tang, R. Muchakayala, S. Song, M. Wang, K.N. Kumar, *Polym. Test*. 50 (2016) 247–254.
3. V.Y. Savitha R, *J. Microb. Biochem. Tech*. 3 (2011) 99–105.
4. S.G. Rathod, R.F. Bhajantri, V. Ravindrachary, P.K. Pujari, G.K. Nagaraja, J. Naik, V. Hebbar, H. Chandrappa, *Bull. Mater. Sci*. 38 (2015) 1213–1221.
5. S. Rajendran, M. Sivakumar, R. Subadevi, *Mater. Lett*. 58 (2004) 641–649.
6. A. Dufresne, Nanocellulose: From nature to high performance tailored materials, 2. Edition, 2017.
7. D. Trache, A. Donnot, K. Khimeche, R. Benelmir, N. Brosse, *Carbohydr. Polym*. 104 (2014) 223–230.
8. P. Murugan, L. Han, C.Y. Gan, F.H.J. Maurer, K. Sudesh, *J. Biotechnol*. 239 (2016) 98-105.
9. M.H. Hussin, A.A. Rahim, M.N. Mohamad Ibrahim, N. Brosse, *Ind. Crops Prod*. 49 (2013) 23–32.
10. Y.P. Timilsena, C.J. Abeywickrama, S.K. Rakshit, N. Brosse, *Bioresour. Technol*. 135 (2013) 82–88.
11. D. Trache, M.H. Hussin, M.K.M. Haafiz, V.K. Thakur, *Nanoscale*. 9 (2017) 1763–1786.
12. Y.N. Sudhakar, M. Selvakumar, *Electrochimica Acta*. 78 (2012) 398–405.
13. M.K. Mohamad Haafiz, S.J. Eichhorn, A. Hassan, M. Jawaid, *Carbohydr. Polym*. 93 (2013) 628–634.
14. R.G. Zhbankov, *New York: Plenum Publishing Corporation*. (1995).
15. S.M.L. Rosa, N. Rehman, M.I.G. De Miranda, S.M.B. Nachtigall, C.I.D. Bica, *Carbohydr. Polym*. 87 (2012) 1131–1138.
16. R. Li, J. Fei, Y. Cai, Y. Li, J. Feng, J. Yao, *Carbohydr. Polym*. 76 (2009) 94–99.
17. F. Fahma, S. Iwamoto, N. Hori, T. Iwata, A. Takemura, *Cellulose*. 17 (2010) 977–985.
18. A. Alemdar, M. Sain, *Bioresour. Technol*. 99 (2008) 1664–1671.
19. M.B. Foston, C.A. Hubbell, A.J. Ragauskas, *Materials*. 4 (2011) 1985–2002.
20. P.T. Larsson, U. Westermark, T. Iversen, *Carbohydr. Res*. 278 (1995) 339–343.
21. R.H. Newman, J.A. Hemmingson, *Cellulose*. 2 (1995) 95–110.